# Molecular Interplay at the PMMA Dielectric and $C_{13}$-BTBT Semiconductor Interface

## Supplementary Information

Kirill Gubanov [1]#, Dustin Vivod [2]#, Christiane Sauer[1], Maria Brzhezinskaya[3], Dirk Zahn[2] and Rainer H. Fink[1]*

[1] Department of Chemistry and Pharmacy, Friedrich-Alexander-Universität Erlangen-Nürnberg, Egerlandstraße 3, 91058 Erlangen, Germany

[2] Computer-Chemie-Centrum and Chair of Theoretical Chemistry, Friedrich-Alexander-Universität Erlangen-Nürnberg, Nägelsbachstraße 25, 91052 Erlangen, Germany

[3] Helmholtz-Zentrum Berlin für Materialien und Energie, Albert-Einstein-Straße 15, 12489 Berlin, Germany

[4] Department of Chemistry and Pharmacy, Friedrich-Alexander-Universität Erlangen Nürnberg, Egerlandstraße 3, 91058 Erlangen, Germany; Interdisciplinary Center for Molecular Materials (ICMM), Friedrich-Alexander-Universität Erlangen-Nürnberg, Egerlandstraße 3, 91058 Erlangen, Germany

**#authors contributed equally**

***corresponding author:** rainer.fink@fau.de

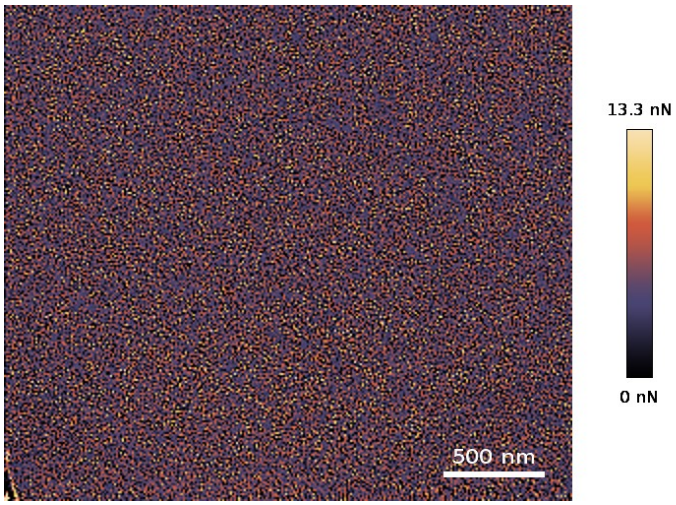


**Fig. S1**: AFM micrograph of the LB-prepared PMMA multilayer adhesion map.

## Methods

### 2.1 Molecule setup

#### 2.1.1 $C_{13}$-BTBT

$C_{13}$-BTBT molecules were geometrically optimized using Gaussian 16 at the B3LYP level of theory using the Def2TZVPP basis set.[1] Afterwards a HF single point calculation was performed with the same basis set to generate the electrostatic potential. With the potential a RESP fit was performed using

antechamber as a part of the AmberTools to generate the point charges for each atom.[2] The Lennard-Jones and bonding parameters of the molecules are derived from the General AMBER Force Field (GAFF) version 1.81.[3]

### 2.1.2 PMMA

The setup of the PMMA was done analogous to the tutorial described by Li.[4] In short similar Gaussian calculations as described above are performed to derive the partial charges of PMMA monomers which are then linked together, here an arbitrary chain length of 60 units was chosen. Once again, all other force field parameters to describe the final molecule are derived from the GAFF.

## 2.2 Slab/Film setup

Molecular dynamics simulations were performed using LAMMPS with a 12 Å cutoff for the evaluation of Lennard-Jones interactions.[5–7] Long-range electrostatics were considered by the PPPM method using a slab correction for 2D periodic systems as part of the ELECTRODE package of LAMMPS with an accuracy of $1.0e^{-4}$ using the same 12 Å cutoff.[8] A timestep of 1 fs was used and temperature control was performed via a Nosé-Hoover style chain thermostat with a relaxation constant of 0.5 ps. Pressure control in X and Y direction was done with a Nosé-Hoover style barostat with a relaxation time of 5 ps.

### 2.2.1 $C_{13}$-BTBT

The $C_{13}$-BTBT film was setup by arranging 400 molecules in a rectangular 20x20 grid of 5.9 x 7.5 Å spacing. This grid was then heated up to 300 K with a rate of 100 K $ns^{-1}$. Afterwards 10 ns at 300K were used to equilibrate the film. During these simulations 2D boundary conditions in X and Y direction were enforced and the same pressure control as described above was applied. Afterwards the periodic boundary conditions were removed by unwrapping the system. This was done to allow for future placement atop the much larger PMMA substrate.

### 2.2.2 PMMA

The PMMA substrate was setup from 64 strands of the 60 chain length long PMMA molecules by replicating the original molecule in X and Y direction 8 times each. The resulting simulation box was then heated up from 600 K to 1000 K over 2 ns. During this time two walls were applied to the system. The first wall at the top of the simulation cell with LJ type interactions using the Sp3 carbon parameters of the GAFF. The second wall was a piston type wall that started from the bottom of the simulation cell and moved upwards. This was done to compress the slab to the desired size of 2.3 nm. Afterwards the bottom wall was changed to the same LJ type wall as the top wall. The slab was simulated for 4 ns at 1000 K before cooling down to 300 K over 3 ns. During these simulations the same 2D boundary conditions in X and Y direction were enforced and pressure control was applied. Afterwards the system was equilibrated for further 22.5 ns after which the final average dimensions of 1.73 nm x 1.98 nm x 2.31 nm were used for further simulations.

### 2.2.3 $C_{13}$-BTBT – PMMA

With the film and slab generated the two systems were merged into one simulation cell by placing the $C_{13}$-BTBT film atop the PMMA substrate. Here, two different setups were created. In the first setup the BTBT unit is in contact to the PMMA substrate and in the other setup the $C_{13}$ alkyl chain is in contact to the PMMA substrate. Each setup consisted of four further subsetups, with two subsetups per side of the PMMA substrate, which differ by a 90° rotation of the BTBT film.

## 2.3 Productions runs

These systems were then simulated for 40 ns in the canonical ensemble at 300 K with the same thermostat as described above. The first 20 ns were seen as equilibration and the last 20 ns were used as production for analysis. Equilibration was determined by Gaussian fits of the potential energy of the system. Due to the size of the BTBT film edge effects have a large contribution in the energies of the system. In order to reduce this influence in the analysis a subgroup of BTBT molecules, denoted as core, was used for analysis. For this analysis the other $C_{13}$-BTBT molecules have been removed from the trajectories and reruns, using the coordinates of the productions runs, with these reduced trajectories have been carried out.

### 2.3.1 Adsorption energy

To extract the adsorption energy of the BTBT film onto the PMMA substrate the following formula was used:

$$E_{ads} = \langle E_{BTBT-PMMA}^{core} - \left(E_{PMMA} + E_{BTBT}^{core}\right)\rangle_t \qquad (1)$$

where $E_{ads}$is the adsorption energy, $E_{BTBT-PMMA}^{core}$ is the potential energy of the system containing the PMMA substrate and the BTBT core molecules, and $E_{PMMA}$ and $E_{BTBT}^{core}$ are the system containing only the PMMA substrate and the BTBT core molecules respectively. **Fig. S2** shows a scheme depicting the used deconstructed trajectories. It is further possible to split the potential energy into its Lennard-Jones and electrostatic components.

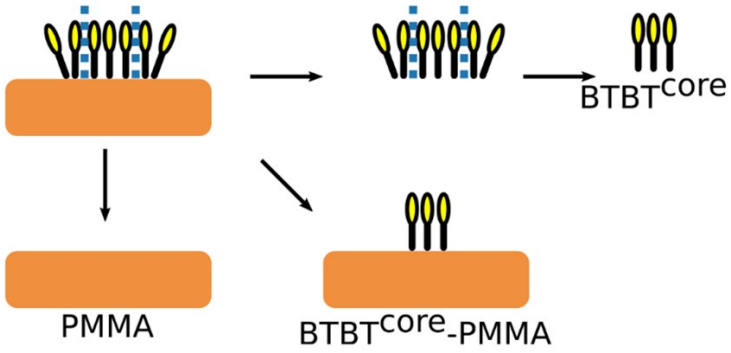


**Fig. S2**: Scheme depicting the deconstructed systems starting from the full system shown in the top left. PMMA substrate shown in orange, and BTBT molecules shown as black and yellow 'sticks'. Blue dashed lines show the core molecules.

### 2.4 Voronoi

In order to evaluate the area of the different $C_{13}$-BTBT configurations 2D Voronoi analysis has been performed using the SciPy module.[9] For each setup the average positions of the $C_{13}$-BTBT molecules was used. The resulting areas are plotted in **Fig. S3**.

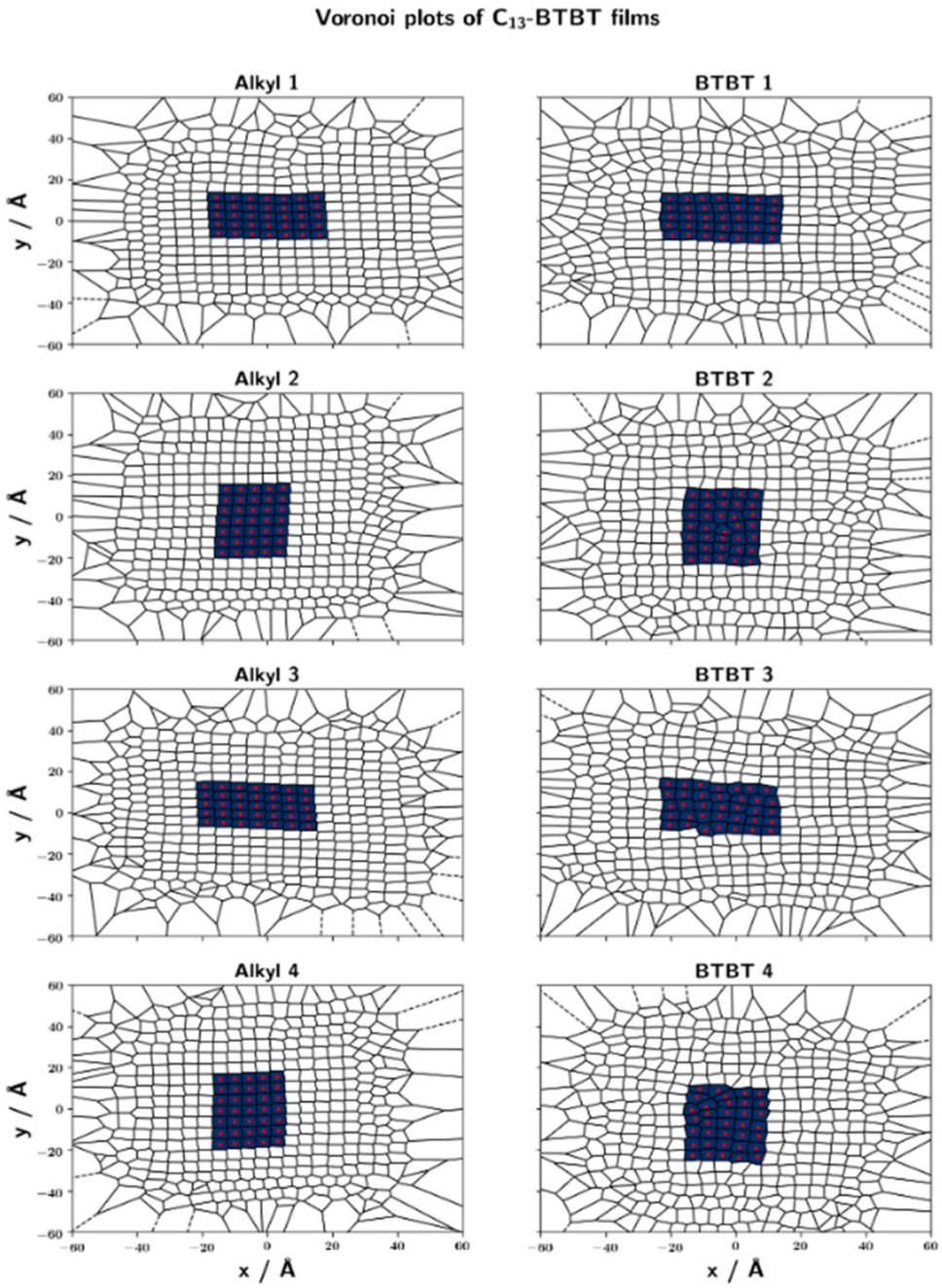


**Fig. S3**: Voronoi plots of the different C13-BTBT films. Blue areas are the areas of the core molecules used, with the molecules being shown as red dots.

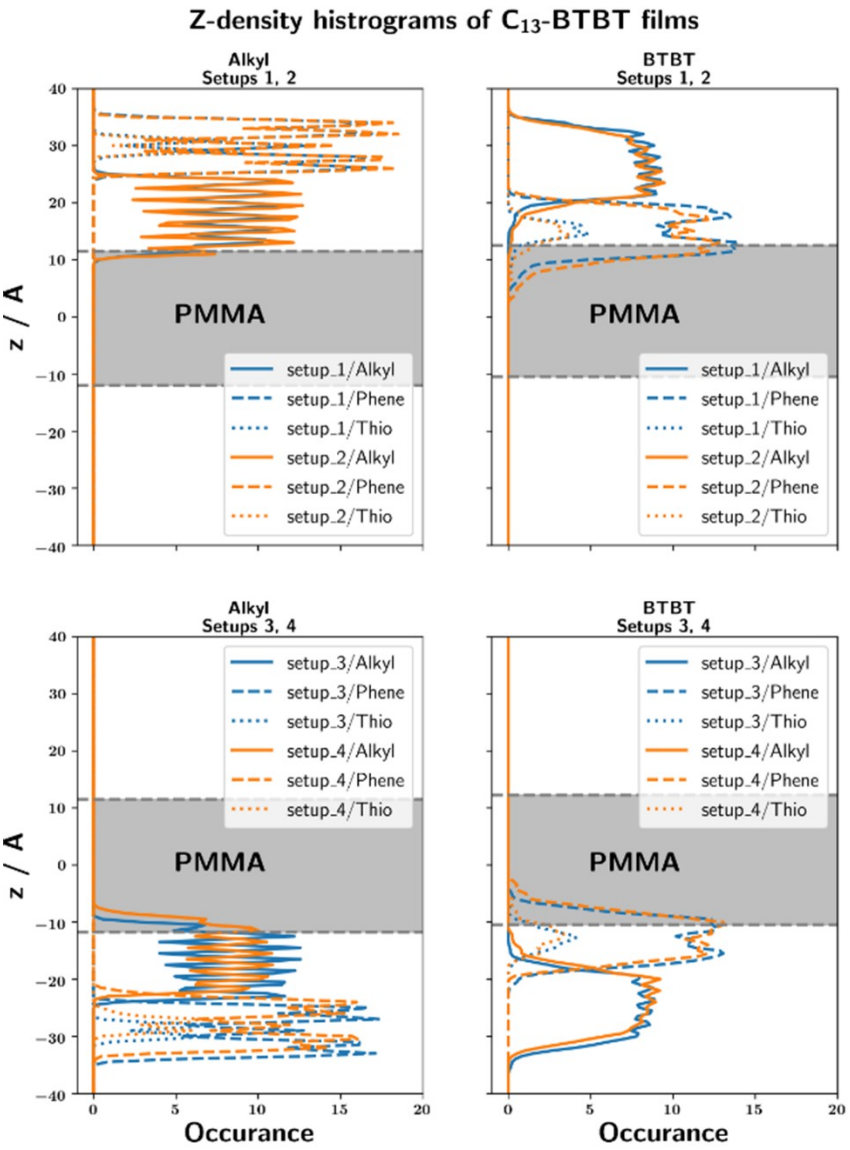


**Fig. S4**: Histograms of z-positions for each setup.

## SI References

1 M. J. Frisch, G. W. Trucks, H. B. Schlegel, G. E. Scuseria, M. A. Robb, J. R. Cheeseman, G. Scalmani, V. Barone, G. A. Petersson, H. Nakatsuji, X. Li, M. Caricato, A. V. Marenich, J. Bloino, B. G. Janesko, R. Gomperts, B. Mennucci, H. P. Hratchian, J. V. Ortiz, A. F. Izmaylov, J. L. Sonnenberg, D. Williams-Young, F. Ding, F. Lipparini, F. Egidi, J. Goings, B. Peng, A. Petrone, T. Henderson, D. Ranasinghe, V. G. Zakrzewski, J. Gao, N. Rega, G. Zheng, W. Liang, M. Hada, M. Ehara, K. Toyota, R. Fukuda, J. Hasegawa, M. Ishida, T. Nakajima, Y. Honda, O. Kitao, H. Nakai, T. Vreven, K. Throssell, J. A. Montgomery Jr., J. E. Peralta, F. Ogliaro, M. J. Bearpark, J. J. Heyd, E. N. Brothers, K. N. Kudin, V. N. Staroverov, T. A. Keith, R. Kobayashi, J. Nor mand, K. Raghavachari, A. P. Rendell, J. C. Burant, S. S. Iyengar, J. Tomasi, M. Cossi, J. M. Millam, M. Klene, C. Adamo, R. Cammi, J. W. Ochterski, R. L. Martin, K. Morokuma, O. Farkas, J. B. Foresman and D. J. Fox, *Gaussian˜16 Revision C.01*, Gaussian Inc. Wallingford CT, 2016.

2 J. Wang, W. Wang, P. A. Kollman and D. A. Case, *J. Mol. Graph. Model*., 2006, **25**, 2, 247–260. https://doi.org/10.1016/j.jmgm.2005.12.005

3 J. Wang, R. M. Wolf, J. W. Caldwell, P. A. Kollman and D. A. Case, *J. Comput. Chem*., 2004, **25**, 1157–1174. https://doi.org/10.1002/jcc.20035

4 P. Li, "*Amber advanced tutorial*", 27, can be found under https://ambermd.org/tutorials/advanced/tutorial27/pet.php, (Accessed: 2023-09-15).

5 A. P. Thompson, H. M. Aktulga, R. Berger, D. S. Bolintineanu, W. M. Brown, P. S. Crozier, P. J. in 't Veld, A. Kohlmeyer, S. G. Moore, T. D. Nguyen, R. Shan, M. J. Stevens, J. Tranchida, C. Trott and S. J. Plimpton, *Comp. Phys. Comm*., 2022, **271**, 108171. https://doi.org/10.1016/j.cpc.2021.108171

6 W. M. Brown, P. Wang, S. J. Plimpton and A. N. Tharrington, *Comput. Phys. Commun*., 2011, **182**, 898–911. https://doi.org/10.1016/j.cpc.2011.10.012

7 W. M. Brown, A. Kohlmeyer, S. J. Plimpton and A. N. Tharrington, *Comput. Phys. Commun.,* 2012, **183**, 449–459. https://doi.org/10.1016/j.cpc.2010.12.021

8 L. J. V. Ahrens-Iwers, M. Janssen, S. R. Tee and R. H. Meißner, *J. Chem. Phys.,* 2022, **157**, 084801. https://doi.org/10.1016/j.cpc.2011.10.012

9 P. Virtanen, R. Gommers, T. E. Oliphant, M. Haberland, T. Reddy, D. Cournapeau, E. Burovski, P. Peterson, W. Weckesser, J. Bright, S. J. van der Walt, M. Brett, J. Wilson, K. J. Millman, N. Mayorov, A. R. J. Nelson, E. Jones, R. Kern, E. Larson, C. J. Carey, ˙ I. Polat, Y. Feng, E. W. Moore, J. VanderPlas, D. Laxalde, J. Perktold, R. Cimrman, I. Henriksen, E. A. Quintero, C. R. Harris, A. M. Archibald, A. H. Ribeiro, F. Pedregosa and P. van Mulbregt, SciPy 1.0 Contributors, *Nat Methods,* 2020, **17**, 261–272. https://doi.org/10.1038/s41592-019-0686-2